

## Oxidation Behavior of $\text{UO}_2$ in Air

Gil Sung You, Keon Sik Kim, Duck Kee Min, Seung Gy Ro,  
and Eun Ka Kim

Korea Atomic Energy Research Institute  
(Received August 3, 1994)

### $\text{UO}_2$ 의 공기중 산화거동

유길성 · 김건식 · 민덕기 · 노성기 · 김은가

한국원자력연구소  
(1994. 8. 3 접수)

#### Abstract

To investigate the storage behavior of the defective LWR spent fuel, air-oxidation tests on non-irradiated and irradiated  $\text{UO}_2$  were performed. The weight gains of non-irradiated  $\text{UO}_2$  specimens are characterized by the S-shape curves at 250-400°C temperature range. One hundred percent conversion of  $\text{UO}_2$  to  $\text{U}_3\text{O}_8$  corresponds with about 4% weight increase. The activation energies are 110 kJ/mol above 350°C and 153 kJ/mol below 350°C. The irradiated  $\text{UO}_2$  specimens with about 35 GWD/MTU burnup were oxidized at 300-400°C in air. They show a rapid increase of weight gain at the initial stage and a slow increase at the later stage when compared with non-irradiated  $\text{UO}_2$ . The activation energy under these conditions is 95 kJ/mol. Burnup and aging effects of irradiated  $\text{UO}_2$  were also investigated at 350°C in air environment, but the specimens appears insensitive to these variables.

#### 요 약

가압 경수로형 결함 핵연료에 대한 장기 저장 거동을 연구하기 위하여 미조사 및 조사된  $\text{UO}_2$ 에 대한 공기 중 산화 시험을 수행하였다. 미조사  $\text{UO}_2$  시편의 산화 시험은 250-400°C 온도 범위의 공기 중에서 수행되었으며 시험결과 전 시험 온도 구간에서 S-곡선의 무게 증가 특성을 보여 주었다. 또한  $\text{UO}_2$ 가  $\text{U}_3\text{O}_8$ 으로 최대 변환될 때의 무게 증가율은 약 4wt% 정도였다. 이 때 활성화 에너지는 350°C 이상에서는 약 110 kJ/mol로 나타났고 350°C 이하에서는 약 153 kJ/mol로 나타났다. 약 35 GWD/MTU으로 연소된 조사  $\text{UO}_2$  시편에 대한 300-400°C 온도 영역에서의 공기 중 산화 시험 결과는 미조사 시편과 비교할 때 초기에는 산화 속도가 빨리 증가하다가 산화가 진행될 수록 산화 속도가 느리게 증가하는 경향을 보여 주었으며 이 때의 활성화에너지는 약 95 kJ/mol로 나타났다. 350°C 공기 분위기에서 연소도와 aging 효과에 대한 시험결과 특별한 산화 거동에서의 차이점을 나타내지 않았다.

## 1. Introduction

When  $\text{UO}_2$  is oxidized in air, it can be transformed into the various meta-stable oxides, such as  $\text{U}_4\text{O}_9$ ,  $\text{U}_3\text{O}_7$  and  $\text{U}_3\text{O}_8$ . Many studies to understand the  $\text{UO}_2$  oxidation behaviors have been performed because of the importance of fuel oxidation in the long-term storage and disposal of spent fuels. When  $\text{UO}_2$  is transformed into tetragonal oxide  $\text{U}_3\text{O}_7$ , the density is changed from  $10.96\text{g/cm}^3$  to  $11.4\text{g/cm}^3$ . The initial volume, therefore, reduces about 2% after the transformation. When  $\text{UO}_2$  is transformed into  $\text{U}_3\text{O}_8$ , having an orthorhombic structure, the density is changed to  $8.35\text{g/cm}^3$ . The volume expands about 30% when compared with that of  $\text{UO}_2$ . In this case, the cladding can be breached by stress build-up caused by the volume expansion of the fuel, and thus the fission gas can release in open space through the cracks. Another important concern for the  $\text{UO}_2$  oxidation is that the oxidation products and resulting physical degradation may affect radionuclide leaching rates for fuel exposed to ground water[1].

In this paper a study of  $\text{UO}_2$  oxidation in air has been conducted for analyses of the long-term storage behavior and accident analysis of fuel rod during both wet and dry storage-conditions. The oxidation behavior of irradiated  $\text{UO}_2$  was compared with that of non-irradiated  $\text{UO}_2$ .

## 2. Experimental Procedures

The non-irradiated  $\text{UO}_2$  specimens were cut from the commercial PWR type  $\text{UO}_2$  pellet. The initial weights of the specimens were about 630mg. The continuous weighing method was used to obtain more accurate data. It was checked and confirmed that thermal cycling effect, which may affect the comparison with the result from the intermittent method on irradiated  $\text{UO}_2$ , can be neglect. Figure 1(a) shows the oxidation test equipment and automatic data acquisition system. The oxidation test was performed by a cylindrical type furnace with a programmable

controller. The pan and extension wire (0.2mm diameter) for hanging samples were made of platinum. The weight gain was measured continuously by Cahn-30 balance with an interface and a data acquisition system. The maximum precision of the balance is  $0.1\mu\text{g}$ .

The oxidation test on irradiated  $\text{UO}_2$  was performed on the fragment specimens taken from KORI-1 PWR fuel using an intermittent weighing method. The fuel had a final discharge burnup of 35 GWD/MTU. It had been cooled for 6 years in storage pool. To know the burnup effect on oxidation of  $\text{UO}_2$ , some different burnup specimens with 13.9 and 39.2 GWD/MTU were used. Density measurement on several specimens from another 7 spent fuel rods were also performed to reveal the relationship between burnup and bulk density of  $\text{UO}_2$ . 15-month ambient air aging specimen was also examined to determine the aging effect. Figure 1(b) shows the equipment of hot cell test for irradiated  $\text{UO}_2$  oxidation. The initial weights of irradiated  $\text{UO}_2$

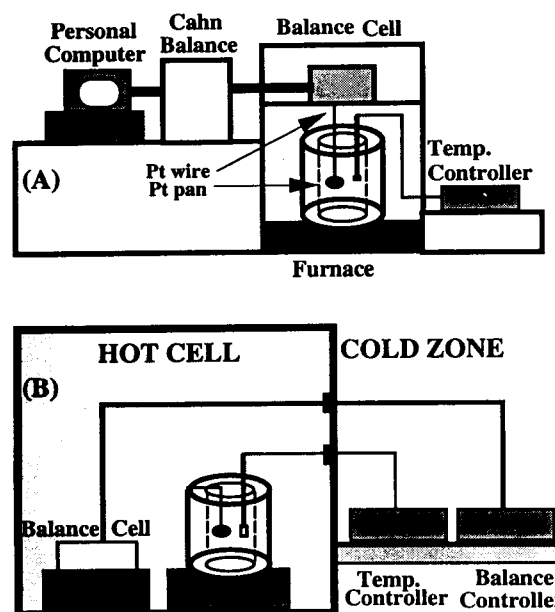


Fig. 1. Test Apparatus of (a) Non-Irradiated  $\text{UO}_2$  and (b) Irradiated  $\text{UO}_2$ .

specimens were about 500mg. The grain size distribution of the specimens was among 7 and  $11\mu\text{m}$ , and the initial average density was  $10.30\text{g}/\text{cm}^3$ .

### 3. Results and Discussion

#### 3.1. Oxidation Behavior of Non-irradiated $\text{UO}_2$

Figure 2 shows the weight gain features of non-irradiated  $\text{UO}_2$  in the temperature range between  $250^\circ\text{C}$  and  $400^\circ\text{C}$ . As shown in this figure, the weight gains of the non-irradiated  $\text{UO}_2$  are characterized by the S-shape curve. The oxidation of  $\text{UO}_2$  proceeds very slowly at the initial stage, and increases linearly at the midterm range. It shows a smooth saturation at the later stage. When 100%

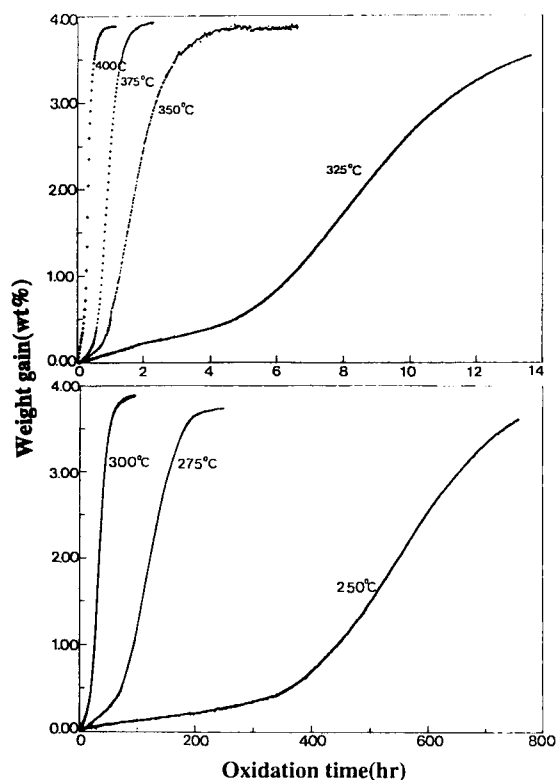


Fig. 2. Weight Gain Characteristics of Non-Irradiated  $\text{UO}_2$  by Air-Oxidation Over the Temperature Range of  $250^\circ\text{C}$  to  $400^\circ\text{C}$ .

conversion of  $\text{UO}_2$  to  $\text{U}_3\text{O}_8$  occurs, the initial weight is gained about 4wt%. Figure 3 shows the time for about 50% transformation into  $\text{U}_3\text{O}_8$ , comparing with Boase's results[2]. The activation energies(AEs) obtained from Boase's results are  $170\text{ kJ/mol}$  and  $66.5\text{ kJ/mol}$  in the range of  $330\text{--}350^\circ\text{C}$  and  $350\text{--}400^\circ\text{C}$ , respectively. He also suggested the existence of a transition point at  $350^\circ\text{C}$ . The present study, however, shows that the AEs are  $153\text{ kJ/mol}$  in  $250\text{--}350^\circ\text{C}$  and  $109\text{ kJ/mol}$  in  $350\text{--}400^\circ\text{C}$ . Identical to Boase's results, the transition point appeared at about  $350^\circ\text{C}$ . Although the transition point was same, the present study shows lower values of AEs than Boase's.

#### 3.2. Oxidation Behavior of Irradiated $\text{UO}_2$

The weight gains of irradiated  $\text{UO}_2$  in  $300\text{--}400^\circ\text{C}$  in air are plotted in Fig.4. At the initial stage the weight gains increase very fast and seem to be saturated at the point of about 2 wt%. Even though the fabrication history and the oxidation condition of the specimens are different, the weight gain trend is simi-

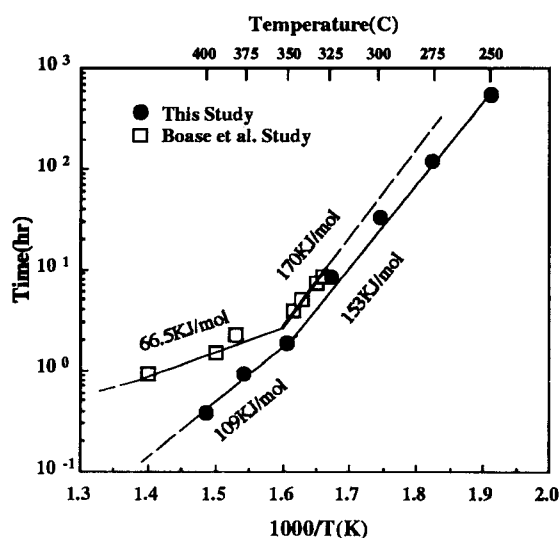


Fig. 3. Comparison Between this Study and Boase's Results for 50% Conversion Time of Non-Irradiated  $\text{UO}_2$ .

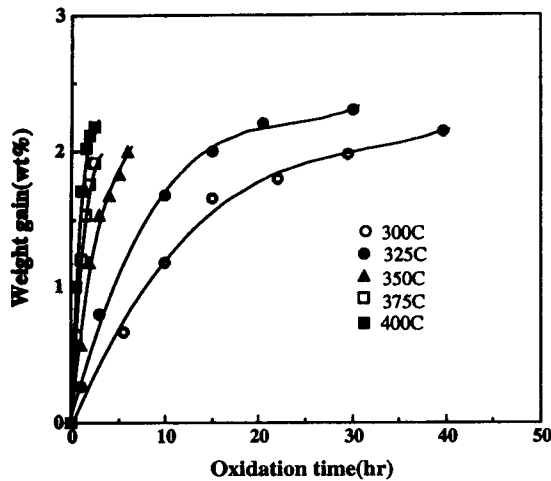


Fig. 4. Weight Gain Characteristics of Irradiated  $\text{UO}_2$  by Air-Oxidation Between 300°C and 400°C.

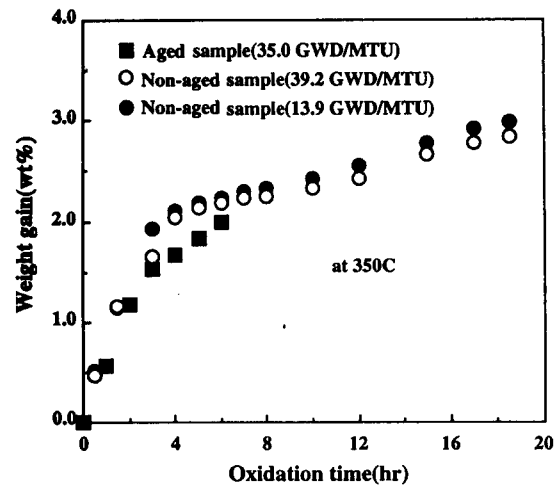


Fig. 6. The Effects of Burnup and Aging on Oxidation of Irradiated  $\text{UO}_2$ .

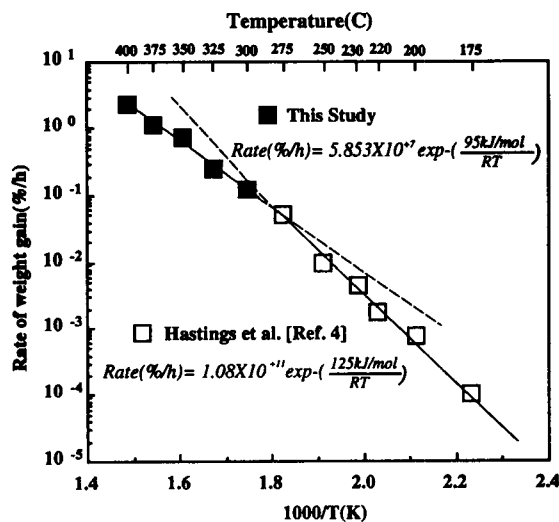


Fig. 5. Rate of Weight Gain Versus  $1/T$  for Irradiated  $\text{UO}_2$  at 300-400°C (This Study) and 175-275°C (Hastings' Study).

lar to Campbell's results[3]. Figure 5 shows the oxidation rate of irradiated  $\text{UO}_2$  as a function of the reciprocal absolute temperature. The oxidation rate increases exponentially with temperature. In the figure 5, the present and Hastings' results[4] for irradiated  $\text{UO}_2$  are shown. The AEs obtained from both results are 95 kJ/mol in 300-400°C and 125

kJ/mol in 175-275°C, respectively. The difference between the present and Hastings' results may be due to the differences of the test conditions, specimen history, shape and size, etc. The effects of burnup and aging on irradiated  $\text{UO}_2$  are also studied at 350°C in air and the results are shown in Fig.6. The effect due to the burnup difference between 13.9 GWD/MTU and 39.2 GWD/MTU seems not to be clear as shown in this figure. The irradiation on  $\text{UO}_2$  is accompanied by density change and generation of many kinds of fission products. It is generally known that the density change and fission products of  $\text{UO}_2$  can affect the oxidation behavior of  $\text{UO}_2$ . The densities for the present work specimens, however, do not show a clear relationship to burnup when considering of the data from the same assembly rods in Fig.7. It may imply that the difference of fission products and/or radiation damages dependent on burnup might not reveal a visible effect on the oxidation of  $\text{UO}_2$ . Campbell[5] says the aging of  $\text{UO}_2$  can make some protection layer on  $\text{UO}_2$  surface and the layer can delay the oxidation rate. In this work, however, the aging effect, as also shown in Fig.6, is not clearly appeared. The absence of aging effect might be explained from the fact that the relatively

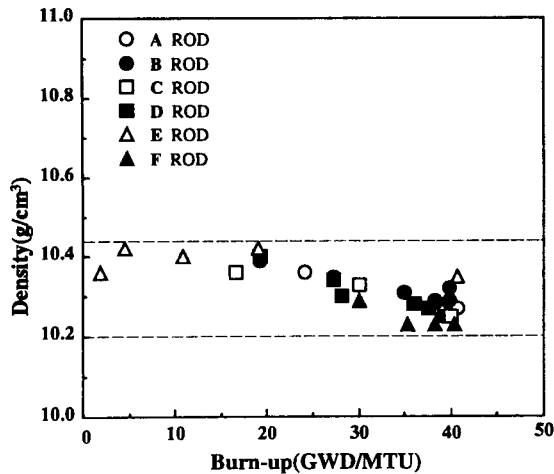
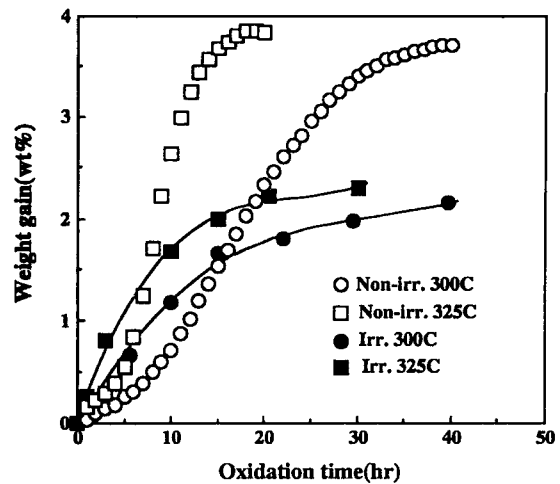


Fig. 7. Dependence of Density on Burnup.

high oxidation temperature could destroy the protection layer produced under relatively low temperature.

### 3.3. Comparison of Oxidation Behavior of Non-irradiated $\text{UO}_2$ with Irradiated $\text{UO}_2$

Figure 8 compares the oxidation behaviors of the non-irradiated and irradiated  $\text{UO}_2$  specimens at 300°C and 325°C in air. In this figure the weight gain curve demonstrates that irradiated  $\text{UO}_2$  oxidation can be significantly differentiated from non-irradiated  $\text{UO}_2$  oxidation. The non-irradiated  $\text{UO}_2$  is oxidized very slow at the early stage of oxidation, while the irradiated  $\text{UO}_2$  is oxidized very fast at this stage. At the later stage of oxidation, contrary to the early stage, a fast oxidation occurred in non-irradiated  $\text{UO}_2$ , but relatively slow oxidation in irradiated one. It has been generally known that many factors may affect the oxidation behavior of  $\text{UO}_2$ . The factors, for example, are fabrication history, oxidation condition, structural changes, fission products, changes of chemical composition and oxygen potential, etc. Some investigators[4] reported that the fabrication history and shape of test specimen did not affect the weight gain characteristics. Einziger[6] reported that irradiated fuel pellet fragments from spent fuel rods

Fig. 8. Comparison of Oxidation Behavior of Irradiated and Non-Irradiated  $\text{UO}_2$  at 300°C and 325°C.

have been converted to  $\text{U}_4\text{O}_9$  without forming  $\text{U}_3\text{O}_7$  or  $\text{U}_3\text{O}_8$ . They also expressed the lack of  $\text{U}_3\text{O}_8$  formation after several years in their tests suggested enhanced oxidation resistance of the fuels following burnup. In the present test, however, the burnup difference did not reveal any effect on the  $\text{UO}_2$  oxidation behavior.

The difference of the oxidation curve shapes between non-irradiated and irradiated  $\text{UO}_2$  might be considered due to the microstructural change by irradiation. During irradiation, the sintering and fission gas pores distributed in  $\text{UO}_2$  grain can migrate into the grain boundaries, and form fission gas bubbles. These bubbles may accelerate the oxidation rate by contributing to the diffusion paths for oxygen. Tomas and Woodley[7, 8] observed the fission gas bubbles of 2-10nm diameter in grain boundaries of irradiated  $\text{UO}_2$ . They explained that the fast oxidation in the initial stage was due to the fast diffusion of oxygen through the bubbles. Campbell[9] also studied the effect of microporosity on the oxidation behavior of  $\text{UO}_2$ . Therefore, the fast and slow oxidation features at the initial and later stages might be explained as follows; At the initial stage the irradiated  $\text{UO}_2$  is oxidized faster by easy diffusion of oxygen through

the bubble inter-linked grain boundaries. In the later stage, however, the possibility of some other phase formation, for example  $U_4O_9$ , etc., may explain the delaying of  $U_3O_8$  formation as well as Thomas' suggestion[1]. For the detail mechanism study of delaying oxidation phenomena at the later stage, more experiments will be needed.

### 3.4. Failure Analysis of Spent Fuel

In order to predict the failure initiation time of spent fuel, the oxidation mechanism must be clear at first. Up to the present, however, there is not enough data to confirm the above mentioned several mechanisms. If the irradiated  $UO_2$  follows the same oxidation behavior with non-irradiated  $UO_2$  conservatively, the time for the 15% conversion of  $UO_2$  into  $U_3O_8$  as a function of the reciprocal temperature can be seen as in Fig.9. When  $UO_2$  is converted into  $U_3O_8$  by 15%, the diameter of fuel rod increases about 2%. It is the design criterion capable of inducing the initiation of fuel rod cracks. The Arrhenius relationships of the 15% conversion to  $U_3O_8$  are given as following equations ;

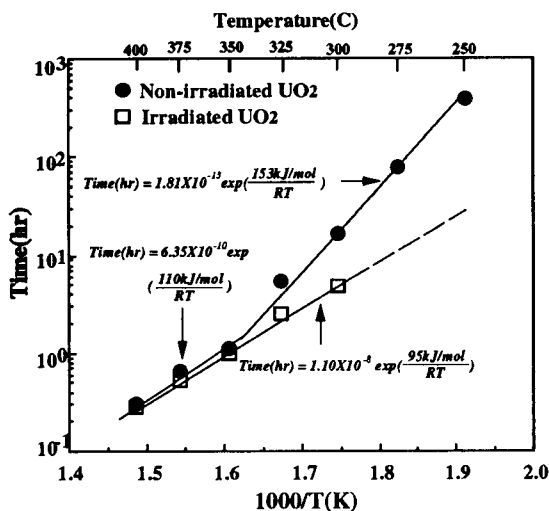


Fig. 9. Relationship Between Time and Temperature of 15% Conversion of  $UO_2$  to  $U_3O_8$ .

$$\log t(\text{hr}) = -12.7 + 8005/T(^{\circ}\text{K}) : \text{non-irradiated specimen at } 250-350^{\circ}\text{C}$$

$$\log t(\text{hr}) = -8.2 + 5813/T(^{\circ}\text{K}) : \text{non-irradiated specimen at } 350-400^{\circ}\text{C}$$

$$\log t(\text{hr}) = -7.9 + 4963/T(^{\circ}\text{K}) : \text{irradiated specimen at } 300-400^{\circ}\text{C}$$

Where  $t$  and  $T$  are the conversion time and the absolute temperature, respectively. By using the above equations, the oxidation periods of 15% conversion of  $UO_2$  to  $U_3O_8$  can be predicted and used for the safety analysis of defective fuel rods during storage. If the oxidation mechanism of irradiated fuel becomes clearer, the above equation obtained from irradiated specimens must be changed by more correct expression.

### 4. Conclusions

From this study on  $UO_2$  oxidation behavior, using non-irradiated and irradiated  $UO_2$ , following conclusions can be drawn :

1. The Arrhenius relationships of 15% conversion of  $UO_2$  to  $U_3O_8$  are given as following equations conservatively ;

$$\log t(\text{hr}) = -12.7 + 8005/T(^{\circ}\text{K}) : \text{non-irradiated specimen at } 250-350^{\circ}\text{C}$$

$$\log t(\text{hr}) = -8.2 + 5813/T(^{\circ}\text{K}) : \text{non-irradiated specimen at } 350-400^{\circ}\text{C}$$

$$\log t(\text{hr}) = -7.9 + 4963/T(^{\circ}\text{K}) : \text{irradiated specimen at } 300-400^{\circ}\text{C}$$

Where  $t$  and  $T$  are the conversion time and the absolute temperature, respectively.

2. In contrast to the non-irradiated  $UO_2$ , irradiated  $UO_2$  shows more rapid increase of oxidation rate at the initial stage and a lower saturation point at the later stage.

3. Oxidation behavior of irradiated  $UO_2$  shows no burnup dependence up to 39.2 GWD/MTU and no aging time dependence on oxidation.

### References

1. L.E. Thomas, R.E. Einziger and H.C. Buchanan, *J. Nucl. Mater.*, **201**, 310 (1993).
2. D.G. Boase, *J. Nucl. Technol.*, **32**, 60 (1977).
3. T.K. Campbell, E.R. Gilbert, and B.J. Wrona, *J. Nucl. Technol.*, **84**, 182 (1989).
4. I.J. Hastings, E. Mizzan and A.M. Ross, *J. Nucl. Technol.*, **68**, 40 (1985).
5. T.K. Campbell, E.R. Gilbert, G.D. White, and G.F. Piepel, *J. Nucl. Technol.*, **85**, 160 (1989).
6. R.E. Einziger, L.B. Thomas, H.C. Buchanan and R.B. Stout, *J. Nucl. Mater.* **190**, 53 (1992).
7. L.E. Thomas and E.R. Gilbert, *Third Inter. Spent Fuel Storage Technol. Symposium*, conf.- 860417-Vol.2 (1986).
8. R.E. Woodley and R.E. Einziger, *J. Nucl. Technol.*, **85**, 74 (1989).
9. T.K. Campbell and E.R. Gilbert, *PNL-6 201*, DE88 000250 (1987).